Nuclear Instruments and Methods in Physics Research B 268 (2010) 3137–3141

Contents lists available at ScienceDirect

Nuclear Instruments and Methods in Physics Research B

journal homepage: www.elsevier.com/locate/nimb

Damage recovery and optical activity in europium implanted wide gap oxides

E. Alves [a,b,*], C. Marques [a,b], N. Franco [a,b], L.C. Alves [a,b], M. Peres [c], M.J. Soares [c], T. Monteiro [c]

[a] Ion Beam Laboratory, Instituto Tecnologico e Nuclear, 2686-953 Sacavém, Portugal
[b] Centro de Fisica Nuclear da Universidade de Lisboa, Lisboa, Portugal
[c] Departamento de Física e I3N, Universidade de Aveiro, 3810-193 Aveiro, Portugal

ARTICLE INFO

Article history:
Received 8 October 2009
Received in revised form 13 May 2010
Available online 25 May 2010

Keywords:
Oxides
Ion implantation
Optical activity
Defect annealing

ABSTRACT

In this study we compare and discuss the defects and optical behaviour of sapphire and magnesium oxide single crystals implanted at room temperature with different fluences (1×10^{15}–1×10^{16} cm^{-2}) of europium ions.

Rutherford backscattering channelling shows that for fluences above 5×10^{15} cm^{-2} the surface disorder level in the Al-sublattice reaches the random level. Implantation damage recovers fast for annealing in oxidizing atmosphere but even for the highest fluence we recover almost completely all the damage after annealing at 1300 °C, independently of the annealing environment (reducing or oxidizing). Annealing above 1000 °C promotes the formation of Eu_2O_3 in the samples with higher concentration of Eu. The optical activation of the rare earth ions at room temperature was observed after annealing at 800 °C by photoluminescence and ionoluminescence. In Al_2O_3 lattice the highest intensity line of the Eu^{3+} ions corresponds to the forced electric dipole $^5D_0 \rightarrow {}^7F_2$ transition that occurs ~616 nm. For the MgO samples the Eu^{3+} optical activation was also achieved after implantation with different fluences. Here, the lanthanide recombination is dominated by the magnetic dipole $^5D_0 \rightarrow {}^7F_1$ transition near by 590 nm commonly observed for samples were Eu^{3+} is placed in a high symmetry local site. The results clearly demonstrate the possibility to get Eu incorporated in optical active regular lattice sites in wide gap oxides.

1. Introduction

Rare-earth (RE) doped insulators are an important class of materials with a wide range of applications in optoelectronic devices, such as optical amplifiers, display phosphors or microlasers with a submicron dimension, etc. This requires that the RE-based materials be synthesized and integrated with functional substrates, such as single crystals, ceramic, nanofibers and other low dimensional structures. A large number of host materials have been studied, from AlN [1,2], SiO_2 [3,4] or Al_2O_3 [5]. Several methods were used to grow the RE doped systems including like radiofrequency (RF) magnetron sputtering [6], sol–gel techniques [7,8], chemical synthesis and deposition [9], co-precipitation [10]. The incorporation of high concentrations of the dopants is limited by the solubility which could be overcome using the ion implantation technique. Ion implantation is a well-established method in semiconductor industry which allows the release of the solid solubility limits and the control of the doping profile. This gives the possibility to tailor the resulting linear and non-linear properties and define the active region of the optical device. However, the intrinsic defects induced by collisions between the incoming particles and the target atoms and/or extrinsic defects resulting from the presence of the implanted ions may hinder the optical activity of the implanted ions. The recovery of the implantation damage and activation of the RE require thermal annealing treatments to allow the relaxation to a stable system [11–13]. We follow the recovery and activation processes in two of the widest band gap oxides, MgO ($E_g \sim 7.8$ eV) and α-Al_2O_3 ($E_g \sim 9$ eV).

Sapphire is by far the most used ceramic, due to its large optical transparency from ultraviolet to near infrared wavelengths, excellent mechanical properties, and good chemical and thermal stability. Similarly, among the variety of RE ions commonly used to dope different kinds of materials, europium ions have tremendous potential due to its strong characteristic red emission for applications in phosphors, electroluminescent devices, optical amplifiers or lasers, and high density optical storage.

In this work 100 keV Eu^+ ions were implanted into α-Al_2O_3 and MgO. The structural and optical changes introduced after implantation and during the thermal annealing treatments up to 1300 °C, in oxidizing and in reducing atmospheres, as well as the lattice site location were studied with Rutherford backscattering channelling (RBS-C) and X-ray diffraction. The optical behaviour was assessed by photoluminescence (PL) and ionoluminescence (IL).

* Corresponding author at: Ion Beam Laboratory, Instituto Tecnologico e Nuclear, 2686-953 Sacavém, Portugal. Tel.: +351 219946086; fax: +351 9941525.
E-mail address: ealves@itn.pt (E. Alves).

0168-583X/$ - see front matter © 2010 Elsevier B.V. All rights reserved.
doi:10.1016/j.nimb.2010.05.072

2. Experimental details

Commercially available MgO(0 0 1) and α-Al_2O_3(0 0 0 1) single crystals were used in these studies. The samples were implanted at room temperature (RT) with 100 keV europium ions. The nominal fluences were in the range of 1×10^{15}–1×10^{16} cm^{-2}. The sapphire samples were tilted 8° to avoid channelling during the implantation while the MgO was implanted normal to the beam (close to the ⟨1 0 0⟩ axis). The expected projected range and straggling of the Eu ions according the SRIM code are 28 and 6 nm, respectively. To recover from the implantation damage thermal annealing was carried out for 1 h in a standard tube furnace at 800, 1000 and 1300 °C in oxidizing (ambient air) and vacuum (2×10^{-4} Pa) atmosphere. Rutherford backscattering channelling (RBS-C) spectrometry studies was performed with a 2.0 MeV He^+ beam after implantation and after each annealing step to characterize the structural changes. The backscattered particles were detected at 140° and close to 180° using silicon surface barrier detectors with resolutions of 13 and 18 keV, respectively. The beam current was measured on the target and kept below 4 nA in order to minimize the effects of charge accumulation at the surface during analysis. Detailed angular scans were performed along the major axial directions to determine the lattice site location of Eu. X-ray diffraction experiments were performed with the Bruker-AXS D8Disvover in θ–2θ Cu K$\alpha_{1,2}$ lines collimated with a Gobël mirror, a Ni filter and a divergent slit of 0.6 mm. A 2θ range from 20° to 100° with a step size of 0.01°, a 0.2 mm detector slit and an acquisition time of 3 s was used. Steady state PL was measured using a Spex 1704 monochromator (1 m, 1200 mm^{-1}) fitted with a cooled Hamamatsu R928 photomultiplier. The samples were mounted in the cold finger of a closed cycle helium cryostat and the sample temperature was controlled in the range from 14 K up to room temperature (RT). A cw He–Cd laser (325 nm line) was used as photon excitation source. Ionoluminescence measurements were done at room temperature using a 1.0 MeV H^+ beam in the range of 200–1100 nm. The current was kept below 1 nA to minimize charge effects and radiation damage.

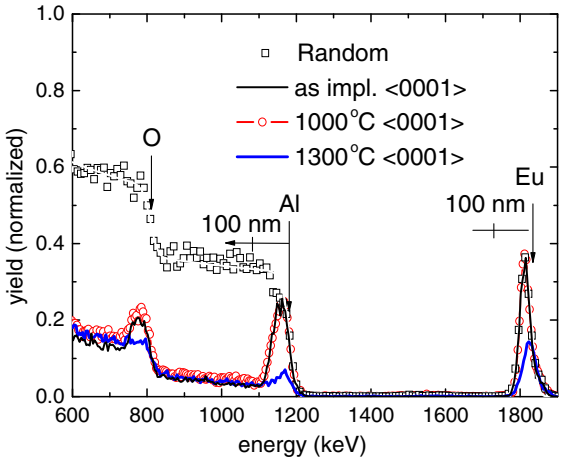

Fig. 1. RBS-C spectra of sapphire implanted with a fluence of 1×10^{16} cm^{-2} annealed for 1 h at 1000 and 1300 °C in oxidizing atmosphere.

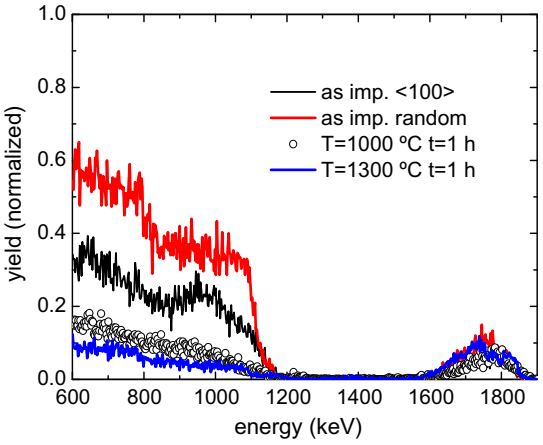

Fig. 2. RBS-C spectra of MgO implanted with a fluence of 1×10^{16} cm^{-2} annealed for 1 h at 1000 and 1300 °C in oxidizing atmosphere.

3. Results

3.1. Structural studies

RBS-C analysis was done after the implantation to assess the implantation damage and the profile of the Eu ions. For the sapphire samples implanted with the lowest fluence (1×10^{15} cm^{-2}) a shallow (40 nm) surface damaged layer is formed (20% minimum yield versus a typical 2% of the unimplanted matrix). Increasing the fluence leads to the widen of the damage layer and for the implantation of 1×10^{16} cm^{-2} the near surface renders amorphous, as the aligned RBS yield from this region overlaps the random, Fig. 1. The high damage level observed at relatively low fluences is related with the chemical reactiveness of Eu, which is known to affect the damage production [12,13]. The europium ions are distributed in a Gaussian profile centred at a range of 25 nm in agreement with SRIM prediction.

Some differences were found for the MgO due to the channelled implantation where a wide and deeper damage profile is observed. Also the Eu profile is much broader compared to the sapphire implantation as expected due to the channelling effect, Fig. 2.

The annealing atmosphere has a role on the system evolution at high temperatures. From our measurements it is evident that the threshold for damage recovery is higher for Al_2O_3. As we can see in Fig. 1 the aligned spectra of Al_2O_3 shows the recrystallization after the annealing at 1300 °C while for MgO (Fig. 2), the recovery happens at 1000 °C. In all the sapphire samples the Eu profile remains unchanged irrespective of the annealing atmosphere and no diffusion or loss of Eu was observed. The formation and stability of Eu ions in the oxide structures can be explained by thermodynamic considerations taking into account the enthalpy of the formation of europium oxides (1662 kJ mol^{-1}) which is close to Al_2O_3 (1690 kJ mol^{-1}) and much higher than MgO (603 kJ mol^{-1}). The presence of europium oxides was confirmed by XRD analyses and the EuO phase was identified in MgO samples after annealing while in sapphire the Eu_2O_3 trivalent phase was dominant, Fig. 3. The formation of these oxide phases has influence on the microstructure evolution and the stability of Eu on laser annealed sapphire implanted with 400 keV Eu ions and the retardation of the α-phase formation up to 1200 °C has been observed by others [14,15].

From the XRD data it is possible to conclude on the crystalline alignment of the RE oxides with the sapphire matrix after annealing, particularly after the annealing at 1300 °C. The ⟨1 1 1⟩ axis of the cubic Eu_2O_3 oxide structure is aligned with the ⟨0 0 0 1⟩ of the corundum structure of Al_2O_3. The crystallographic correlation is clearly seen in the detailed angular scans performed along the normal ⟨0 0 0 1⟩ and tilted ⟨$1\bar{1}01$⟩ shown in Fig. 4. The curve obtained for Eu along the *c*-axis follow the Al curve of the matrix with the same width but a higher minimum yield, χ_{min} (the ratio between the aligned and random yields in the region of analysis).

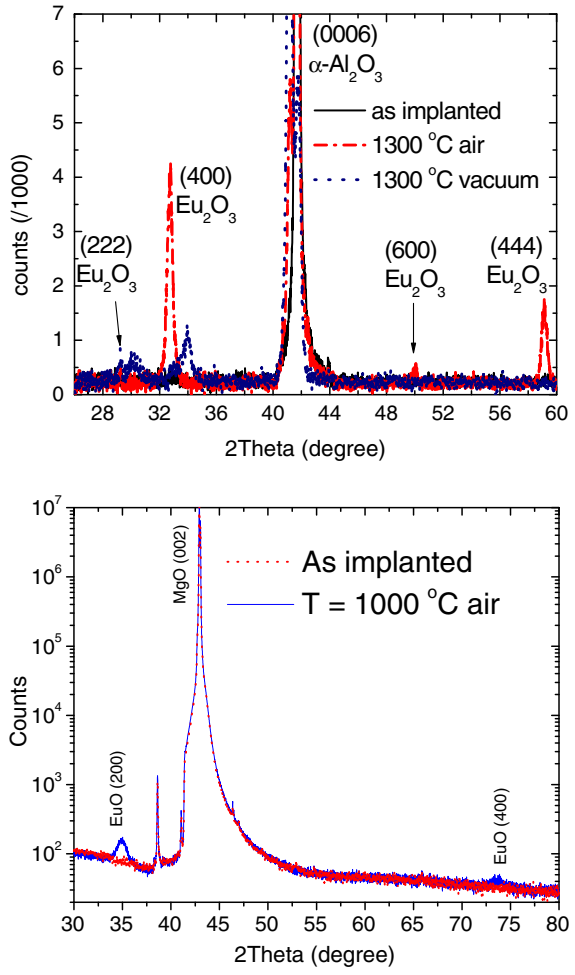

Fig. 3. XRD spectra of sapphire implanted with $1 \times 10^{16}\,cm^{-2}$ (top) and the corresponding for MgO implanted with $1 \times 10^{16}\,cm^{-2}$ (bottom).

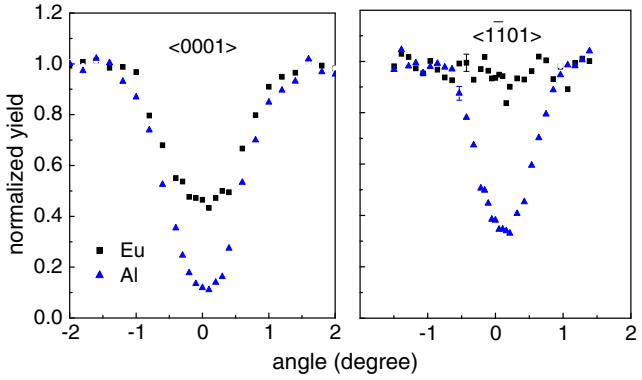

Fig. 4. Detailed angular scans along $\langle 0\,0\,0\,1\rangle$ and $\langle 1\,\bar{1}\,0\,1\rangle$ directions on sapphire implanted with $1 \times 10^{16}\,cm^{-2}$ after annealing in oxidizing atmosphere.

On the contrary along the tilted axis the lanthanide curve is almost flat with some oscillations. This indicates that a large fraction of the Eu ions are incorporated along the $\langle 0\,0\,0\,1\rangle$ direction of the sapphire occupying the distorted vacant regular octahedral site of the corundum structure. The incorporation of REs in distorted octahedral sites was also observed for Er implanted in sapphire [16]. The Er was found 0.8 Å displaced from the ideal octahedral site along the *c*-axis. The reason for this displacement could be related with the difference in the lattice parameters of the two mixed oxides, the corundum Al_2O_3 and Eu_2O_3 C-rare earth type structures [17]. The failure to observe channelling behaviour on Eu implanted MgO after annealing reveal that in this case the RE oxide is not coherent with the matrix. In this case the solubility of both oxides must be very limited since the Eu starts to outdiffuse above 1000 °C as shown in Fig. 2. The segregation of Eu above 1000 °C in (1 0 0) MgO was also studied by Suzuki et al. using ion scattering spectroscopy (ISS) and reflection high energy electron diffraction (RHEED) to study the outmost layers of MgO in ultra high vacuum [18].

3.2. Optical studies

The luminescence characteristics of Eu doped Al_2O_3 and MgO single crystals reveal clear differences which could be directly related to the symmetry of the optical active ions. In Fig. 5 we compare the low temperature PL spectrum of Eu^{3+} ions in MgO and Al_2O_3 after annealing at 1000 °C in air. The emission spectrum of Eu^{3+} ions typically consists on a series of sharp lines in the 570–750 nm wavelength range. For the MgO samples the most intense line occurs ~588 nm and is assigned to the magnetic dipole $^5D_0 \rightarrow {}^7F_1$ transition indicating that the ion is occupying a site with inversion symmetry in the lattice (O_h if Eu replaces for Mg). In the case of sapphire the dominant intra-$4f^6$ recombination arise from transitions between the spin–orbit levels $^5D_0$ and $^7F_2$, at ~616 nm, suggesting the location of Eu^{3+} ion in a lower symmetry site, which is consistent with the RBS/channelling lattice site location. The activation of the implanted ions is achieved after the annealing at 800 °C either in vacuum or oxidizing ambient. Fig. 6(a) shows the 14 K and RT PL spectra for a sapphire sample implanted with $1 \times 10^{15}\,cm^{-2}$ and annealed in air at 1000 °C. Besides the typical impurity related emissions (Cr^{3+} [19] and Fe [20] – related optical centres) the $^5D_0$–$^7F_{J(1-4)}$ Eu^{3+} transitions were assigned. The Eu^{3+} emission is observed up to room temperature (RT) and for all the analysed sapphire samples independently of the used annealing atmosphere. However, the integrated intensity ratio between 14 K and RT varies from 1.25 to 3 indicating that for some samples negligible competitive nonradiative processes occur. In particular, the low thermal quenching was observed for samples annealed in vacuum. Annealing in vacuum also favours the appearance of large unstructured bands in the green (~525 nm) which intensity is seen to decrease for annealing temperatures between 800 and 1300 °C. This band is not present in the samples annealed

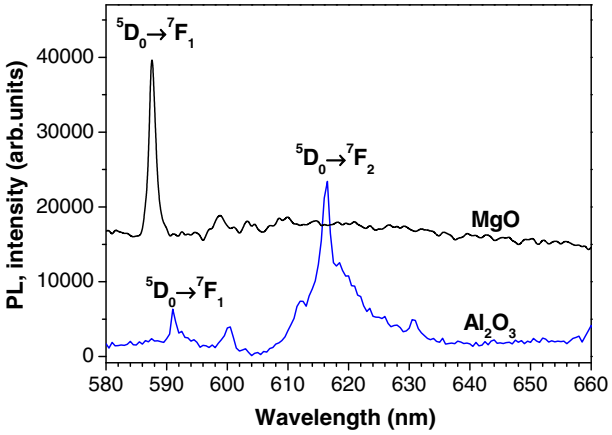

Fig. 5. 14 K PL spectra for the MgO and sapphire samples implanted with 1×10^{15} and $1 \times 10^{16}\,cm^{-2}$ europium ions after annealing at 1000 °C in air. The spectra were obtained with He–Cd (325 nm) excitation.

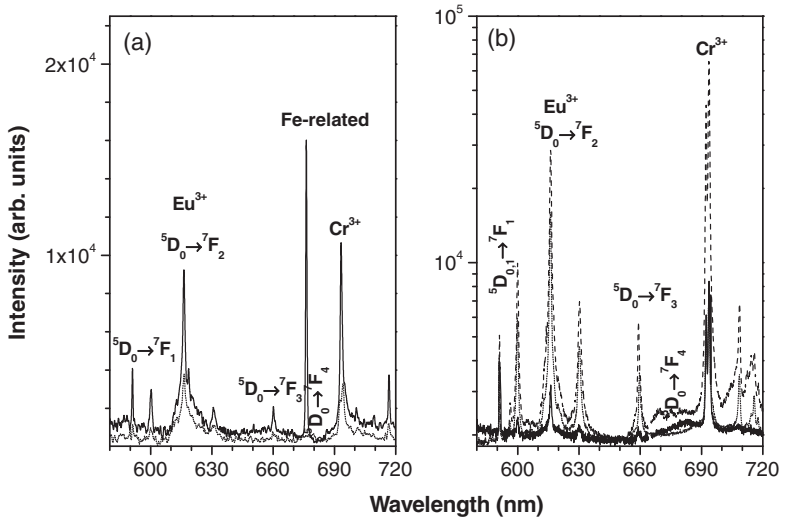

Fig. 6. (a) PL spectra for the sapphire sample implanted with 1×10^{15} cm^{-2} and annealed in air at 1000 °C obtained with He–Cd excitation at 14 K (solid line) and RT (dotted line). (b) RT ionoluminescence for the sample implanted with 1×10^{16} cm^{-2} after implantation (solid line) and annealed at 1300 °C in air (dashed line) and in vacuum (dotted line).

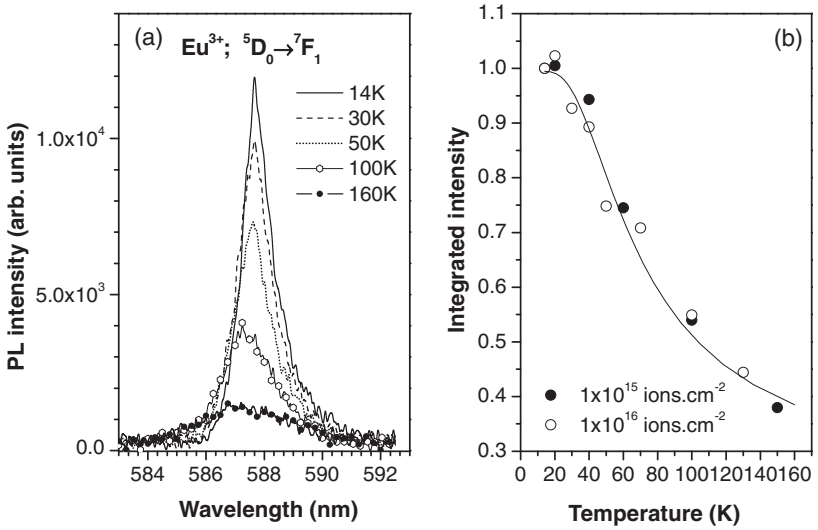

Fig. 7. (a) Temperature dependence of the Eu^{3+} PL intensity for the MgO sample implanted with 1×10^{16} cm^{-2} and annealed in oxidizing atmosphere at 1000 °C. The spectra were obtained with 325 nm excitation and only selected temperatures are shown. (b) Integrated PL intensity as a function of temperature for samples implanted with different fluences.

in air suggesting a possible relation with the presence of metallic reach precipitates in the implanted region. The induced RT Eu^{3+} luminescence by an H^+ beam as excitation source (IL) is shown in Fig. 6(b). These results indicate that Eu^{3+} ions can be optically activated by different excitation paths, using below and above band-gap excitation. Comparing the IL and PL data in the studied wavelength range, no additional optical centres were observed under proton bombardment.

As shown in Fig. 5, the intra-4f^6 emission of Eu^{3+} in MgO samples is dominated by the $^5D_0 \rightarrow {}^7F_1$ transition. In contrast with the observed for the sapphire samples the Eu^{3+} emission cannot be observed up to RT. Fig. 7(a) shows the temperature dependence of the dominant Eu^{3+} transition. From the figure is evident that the intraionic emission is practically absent for temperatures above 180 K. The integrated intensity is well fitted by nonradiative deexcitation processes described by an activation energy of 11.9 ± 1.9 meV.

4. Conclusions

Sapphire single crystals implanted at room temperature with 100 keV europium ions, suffer surface amorphization at 1×10^{16} cm^{-2}. Up to 1000 °C the samples keep the as-implanted profiles unchanged irrespective of the annealing atmosphere. The implantation damage in MgO was reduced due to the channelling effect.

The results reveal the formation of new RE oxide phases during annealing. The Eu_2O_3 observed in Al_2O_3 is coherent with the host matrix. The structure recrystallizes during annealing at 1300 °C

and Eu occupies distorted regular sites along the *c*-axis. The presence of the 3^+ charge state was clearly confirmed by the optical spectra. The intensity of the emission is slightly reduced at room temperature. The major phase found in MgO is EuO and PL results show the incorporation of the optical active ions in high symmetry sites with local inversion. Nonradiative competitive mechanisms are stronger for this wide band gap material than for sapphire as the Eu^{3+} emission is fully quenched above 180 K.

Acknowledgments

We wish to acknowledge Jorge Rocha for the Eu implantation and C. Marques and M. Peres acknowledge FCT for their support through the Ph.D. fellowships SFRH/BD/14276/2003 and SFRH/BD/45774/2008, respectively.

References

[1] K. Lorenz, E. Alves, T. Monteiro, M.J. Soares, M. Peres, P.J.M. Smulders, Nucl. Instrum. Methods B 242 (1–2) (2006) 307–310.
[2] W.M. Jadwisienczak, H.J. Lozykowski, J. Appl. Phys. 89 (8) (2001) 4384.
[3] T. Hayakawa, S.T. Selvan, M. Nogami, Appl. Phys. Lett. 74 (11) (1999) 1513.
[4] N. Can et al., Nucl. Instrum. Methods B 113 (1996) 248.
[5] J. Wrzyszcz et al., J. Alloys Compd. 341 (2002) 358.
[6] M. Losurdo, M. Giangregorio, P. Capezzuto, G. Bruno, M.F. Cerqueira, E. Alves, M. Stepikhova, Appl. Phys. Lett. 82 (18) (2003) 2993–2995.
[7] A.C. Marques, R.M. Almeida, A.R. Ramos, E. Alves, J. Sol–Gel Sci. Technol. 31 (1–3) (2004) 287–291.
[8] M.P.F. Graça, M.A. Valente, M. Peres, A. Cruz, M.J. Soares, A.J. Neves, T. Monteiro, L.C. Alves, E. Alves, J. Phys. – Condens. Matter 19 (1) (2007) 016213.
[9] A. Gedanken et al., Appl. Phys. Lett. 77 (7) (2000) 945.
[10] A.E. Esparza-Garcia, M. Garcıa-Hipólito, M.A. Aguilar-Frutis, C. Falcony, Phys. Status Solidi A 193 (1) (2002) 117.
[11] E. Alves, E. Rita, U. Wahl, J.G. Correia, T. Monteiro, J. Soares, C. Boemare, Nucl. Instrum. Methods B 206 (2003) 1047–1051.
[12] C. Marques, E. Alves, C. McHargue, L.C. Ononye, T. Monteiro, J. Soares, L.F. Allard, Nucl. Instrum. Methods B 191 (2002) 644–648.
[13] E. Alves, M.F. da Silva, J.G. Marques, J.C. Soares, K. Freitag, Nucl. Instrum. Methods B 141 (1998) 353–357.
[14] N. Can, P.D. Townsend, D.E. Hole, C.N. Afonso, Appl. Phys. Lett. 65 (15) (1994) 1871.
[15] O. Ozuna, G.A. Hirata, J. McKittrick, Appl. Phys. Lett. 84 (8) (2004) 1296.
[16] E. Alves, M.F. da Silva, G.N. Van Den Hoven, A. Polman, A.A. Melo, J.C. Soares, Nucl. Instrum. Methods B 106 (1995) 429–432.
[17] F.S. Galasso, Structure and Properties of Inorganic Solids, Pergamon Press, 1970.
[18] T. Suzuki, S. Hishita, K. Oyoshi, R. Souda, Surf. Sci. 391 (1997) 1243–1248.
[19] W.H. Fonger, C.W. Struck, Phys. Rev. B 11 (1975) 3251.
[20] T. Monteiro, C. Boemare, M.J. Soares, E. Alves, C. Marques, C. McHargue, L.C. Ononge, L.F. Allard, Nucl. Instrum. Methods B 191 (2002) 638–643.